DOI 10.1002/mnfr.200800288 Mol. Nutr. Food Res. 2009, *53*, 826 – 835

Research Article

Shallot and licorice constituent isoliquiritigenin arrests cell cycle progression and induces apoptosis through the induction of ATM/p53 and initiation of the mitochondrial system in human cervical carcinoma HeLa cells

Ya-Ling Hsu[1], Chun-Chieh Chia[2], Ping-Jye Chen[2], Su-Er Huang[2], Soon-Cen Huang[2] and Po-Lin Kuo[3, 4]

[1] Graduate Institute of Medicine, Kaohsiung Medical University, Kaohsiung, Taiwan
[2] Department of Obstetrics and Gynecology, Chi Mei Hospital, Liou Ying, Tainan, Taiwan
[3] Institute of Clinical Medicine, Kaohsiung Medical University, Kaohsiung, Taiwan
[4] Department of Medical Research, Kaohsiung Medical University Hospital, Kaohsiung, Taiwan

This study is the first to investigate the anticancer effect of isoliquiritigenin (ISL) in human cervical carcinoma HeLa cells. The results reveal that ISL inhibits HeLa cells by blocking cell cycle progression in the G2/M phase and inducing apoptosis. Blockade of cell cycle is associated with increased activation of ataxia telangiectasia-mutated (ATM). Activation of ATM by ISL phosphorylated p53 at Serine15, resulting in increased stability of p53 by decreasing p53 and murine double minute-2 (MDM2) interaction. In addition, ISL-mediated G2/M phase arrest was also associated with decreases in the amounts of cyclin B, cyclin A, cdc2, and cdc25C, and increases in the phosphorylation of Chk2, cdc25C, and cdc2. The specific ATM inhibitor caffeine significantly decreased ISL-mediated G2/M arrest by inhibiting the phosphorylation of p53 (Serine15) and Chk2. ISL induced apoptotic cell death is associated with changes in the expression of Bax and Bak, decreasing levels of Bcl-2 and Bcl-X_L, and subsequently triggering mitochondrial apoptotic pathway. In addition, pretreatment of cells with caspase-9 inhibitor blocked ISL-induced apoptosis, indicating that caspase-9 activation is involved in ISL-mediated HeLa cell apoptosis. These findings suggest that ISL may be a promising chemopreventive agent against human uterine cervical cancer.

Keywords: Apoptosis / ATM / Cell cycle / Isoliquiritigenin / p53

Received: July 8, 2008; revised: September 6, 2008; accepted: October 8, 2008

1 Introduction

Uterine cervical cancer is still the second most common cancer for women worldwide, despite the existence of effective screening methods [1, 2]. This pathology is currently controlled by surgery and radiotherapy, and is frequently supported by adjuvant chemotherapies [3, 4]. However, currently available chemotherapeutics yield only modest increases in the 5-year survival rate among those patients with advanced cervical cancer, due to the decreased chemosensitivity of cervical cancer cells to chemotherapeutics [3 – 5]. Effective chemopreventive treatment for cervical cancer would have a tremendous impact on cervical cancer morbidity and mortality rate.

Ataxia telangiectasia-mutated (ATM) is phosphoinositide 3-kinase-related kinases (PIKK) that play important, central roles in cellular biology, including cell proliferation and DNA repair [6, 7]. Kinase activity of ATM is induced in response to DNA damage dependent or independent events, then targets several regulators of cell cycle checkpoint and

Correspondence: Dr. Po-Lin Kuo, Institute of Clinical Medicine, College of Medicine, Kaohsiung Medical University, No. 100, Shih-Chuan 1st Road, Kaohsiung 807, Taiwan
E-mail: kuopolin@seed.net.tw
Fax: +886-7-321-0701

Abbreviations: ATM, ataxia telangiectasia-mutated; **ISL,** isoliquiritigenin; **JC-1,** 5,5′,6,6′-tetrachloro-1,1′,3,3′-tetraethylbenzimidazolylcarbocyanine iodide; **MDM2,** murine double minute-2; **PI,** propidium iodide; **TUNEL,** terminal deoxynucleotidyl transferase-mediated deoxyuridine triphosphate nick endlabeling; **XTT,** sodium 3-[1-(phenylamino-carbonyl)-3,4-tetrazolium]-bis(4-methoxy-6-nitro)benzene-sulfonic acid hydrate

cell death [7 – 9]. During this process, ATM undergoes autophosphorylation on Ser1981 and is recruited to sites of DNA damage, where it initiates a signaling cascade through phosphorylation of multiple DNA damage response and cell-cycle proteins, including p53, Chk1/2, and breast cancer 1 and E3 ubiquitin ligases such as murine double minute-2 (MDM2) and constitutively photomorphogenic 1 (COP1) [8, 10, 11]. The tumor suppressor protein p53 is targeted by a wide variety of intracellular and extracellular stimuli, such as withdrawal of growth factors, hypoxia, irradiation, chemicals, and defects in nucleotide synthesis [12, 13]. The activation of p53 leads, primarily through its transcriptional function, to either apoptosis, eliminating those cells harboring severely damaged DNA, or growth arrest, allowing damaged DNA to be repaired and thereby suppressing tumor formation [12, 13]. Stability and activity of p53 are believed to be regulated in part by posttranslational modifications, such as phosphorylation and acetylation [8, 12, 14]. Phosphorylation on NH_2-terminal residues, especially Ser15, Thr18, Ser20, and Ser37, is believed to affect interaction with the negative regulator MDM2 and hence contribute to the stabilization of p53 [8, 14]. Phosphorylation on COOH-terminal Ser315 and Ser392 in particular is believed to enhance the specific DNA binding of p53 *in vitro* [8, 15].

Isoliquiritigenin (ISL), a flavonoid found in licorice (legume) and shallot (liliaceae), is a potent antioxidant with anti-inflammatory, antiplatelet aggregation and cancer-preventing properties [16 – 20]. It exhibits an inhibitory effect on skin and colon carcinogenesis, and antiproliferation activity in liver, pulmonary, prostate, breast, gastric cancer cells [20 – 26]. In this study, we employed the human cervix HeLa adenocarcinoma cell line to assess the molecular mechanisms responsible for the antiproliferative effect of ISL. We found that ISL caused cell cycle arrest at the G2/M phase and induced an apoptotic response.

2 Materials and methods

2.1 Chemicals and reagents

Fetal bovine serum (FBS) and DMEM were obtained from Gibco BRL (Gaithersburg, MD). DMSO, ribonuclease (RNase), and propidium iodide (PI) were purchased from Sigma Chemical (St. Louis, MO). The antibodies to p53, phospho-p53, p21, ATM, phospho-ATM, phospho-H2A.X, NBS1, phospho-NBS1, Chk2, phospho-Chk2, cyclin B, cyclin A, cdc2, cdc25C, phospho-cdc2, phospho-cdc25C, Bax, Bak, Bcl-2, Bcl-X_L, and β-actin were obtained from Cell Signaling Technology (Beverly, MA).

2.2 Cell culture

HeLa (American Type Culture Collection (ATCC) CCL185) was maintained in DMEM supplemented with 10% FBS, 10 U/mL of penicillin, 10 μg/mL of streptomycin, and 0.25 μg/mL of amphotericin, and was cultured in a monolayer culture at 37°C and 5% CO_2.

2.3 Cell proliferation and clonogenic assay

Inhibition of cell proliferation by ISL was measured by XTT (sodium 3′-[1-(phenylamino-carbonyl)-3,4-tetrazolium]-bis(4-methoxy-6-nitro)benzene-sulfonic acid hydrate) assay. Briefly, cells were plated in 96-well culture plates (1×10^4 cells/well), and after 24 h incubation, treated with vehicle alone (0.1% DMSO) and various concentrations of ISL for 48 h. XTT test solution (150 μL), which was prepared by mixing 5 mL of XTT-labeling reagent with 100 μL of electron coupling reagent, was then added to each well. After 4 h of incubation, absorbance was measured on an ELISA reader (Multiskan EX, Labsystems) at a test wavelength of 492 nm and a reference wavelength of 690 nm.

To determine the long-term effects, cells were treated with vehicle alone (0.1% DMSO) and various concentrations of ISL for 1 h. After being rinsed with fresh medium, cells were allowed to grow for 14 days to form colonies that were then stained with crystal violet (0.4 μg/L; Sigma).

2.4 Cell cycle analysis

To analyze cell cycle distribution, 5×10^5 cells were plated in 60 mm dishes and treated with vehicle alone (0.1% DMSO) and ISL (10 and 20 μM) for 6 h. After treatment, the cells were collected by trypsinization, fixed in 70% ethanol, washed in PBS, resuspended in 1 mL of PBS containing 1 mg/mL RNase and 50 μg/mL PI, incubated in the dark for 30 min at room temperature, and analyzed by EPICS flow cytometer. The data were analyzed using Multicycle software (Phoenix Flow Systems, San Diego, CA).

2.5 Apoptosis assay

Apoptotic cells were quantitatively carried out by the terminal deoxynucleotidyl transferase-mediated deoxyuridine triphosphate nick endlabeling (TUNEL) method, which examines DNA-strand breaks during apoptosis by using BD ApoAlert™ DNA Fragmentation Assay kit. Briefly, cells were incubated with vehicle alone (0.1% DMSO) and ISL (10 and 20 μM) for the indicated times. The cells were trypsinized, fixed with 4% paraformaldehyde, and permeabilized with 0.1% Triton X-100 in 0.1% sodium citrate. After being washed, the cells were incubated with the reaction mixture for 60 min at 37°C. The stained cells were then analyzed with an EPICS flow cytometer and a fluorescence microscope at 20 × magnification.

Quantitative analysis of apoptosis was also analyzed by an Annexin V assay kit (BD Biosciences PharMingen, San Jose, CA, USA). Briefly, ISL-treated cells were harvested with trypsin and washed in PBS. Cells were then resuspended in

binding buffer (10 mmol/L HEPES/NaOH (pH 7.4), 140 mmol/L NaCl, 2.5 mmol/L $CaCl_2$) and stained with Annexin V-FITC and PI at room temperature for 15 min in the dark. Cells were then analyzed in an EPICS flow cytometer (Coulter Electronics). Apoptotic cells were defined as Annexin V-FITC-positive and PI-negative cells.

2.6 Assay for caspase-9 activity

The assay is based on the ability of the active enzyme to cleave the chromophore from the enzyme substrate of caspase-9, LEHD-pNA (Ac-Leu-Glu-His-Asp-*p*NA) (Calbiochem, Cambridge, MA). Cell lysates were incubated with peptide substrate in assay buffer (100 mM NaCl, 50 mM HEPES, 10 mM DTT, 1 mM EDTA, 10% glycerol, 0.1% CHAPS, pH 7.4) for 2 h at 37°C. The release of *p*-nitroaniline was monitored at 405 nm. Results are represented as the percentage of change in activity compared to the untreated control.

2.7 Mitochondrial membrane potential assay

We used mitochondrial-specific cationic dye JC-1 (5,5′,6,6′-tetrachloro-1,1′,3,3′-tetraethylbenzimidazolylcarbocyanine iodide) (Molecular Probes), which undergoes potential-dependent accumulation in the mitochondria. Cells were seeded in a 96-well plate. Following treatment with ISL (10 and 20 μM) for the indicated times, cells were stained with 25 μM JC-1 for 30 min at 37°C. Fluorescence was monitored with the fluorescence plate reader at wavelengths of 490 nm (excitation)/540 nm (emission) and 540 nm (excitation)/590 nm (emission) pairs. Changes in the ratio between the measurement at test wavelengths of 590 nm (red) and 540 nm (green) fluorescence intensities are indicative of changes in the mitochondrial membrane potential.

2.8 Immunoblot/immunoprecipitation

Cells were treated with 20 μM ISL at specified intervals of time. The cells were lysed on ice for 40 min in a solution containing 50 mM Tris, 1% Triton X-100, 0.1% SDS, 150 mM NaCl, 2 mM Na_3VO_4, 2 mM EGTA, 12 mM β-glycerolphosphate, 10 mM NaF, 16 μg/mL benzamidine hydrochloride, 10 μg/mL phenanthroline, 10 μg/mL aprotinin, 10 μg/mL leupeptin, 10 μg/mL pepstatin, and 1 mM PMSF. The cell lysate was centrifuged at $14000 \times g$ for 15 min, and the supernatant fraction was collected for immunoblot. Equivalent amounts of protein were resolved by SDS-PAGE (8 – 12%) and transferred to PVDF membranes. After blocking for 1 h in 5% nonfat dry milk in Tris-buffered saline, the membrane was incubated with the desired primary antibody for 1 – 16 h. The membrane was then treated with appropriate peroxidase-conjugated secondary antibody, and the immunoreactive proteins were detected using an enhanced chemiluminescence kit (Amersham, USA) according to the manufacturer's instructions.

For association of p53 and MDM2, cell lysates (300 μg) were incubated with 10 μL anti-MDM2 for 1 h at 4°C. Immunocomplexes were resolved by 7.5% SDS-PAGE. Association of MDM2 with p53 was detected by incubating the blots with anti-MDM2 and anti-p53 antibodies as described above.

2.9 The p53 activity

p53 activity was determined by ELISA Trans-AM kit used according to the manufacturer's specifications (Active Motif, Carlsbad, CA). Briefly, the transcriptional factor of nuclear extracts, which were prepared by Nuclear Extract kit (Active Motif), were captured by binding to a consensus oligonucleotide (5′- CTTGGACATGCCCGGGCATGTCC CTC-3′) immobilized on a 96-well plate. The amount of p53 was determined in a colorimetric reaction using specific primary antibody and a secondary horseradish peroxidase-conjugated antibody. Spectrophotometric data were expressed as a ratio of absorbance of each experimental condition compared with control cells exposed to vehicle alone [27].

2.10 Stable transfection

Transfection of HeLa cells was carried out using Lipofectamine 2000 reagent (Life Technologies). HeLa cells were exposed to the mixture of Lipofectamine 2000 reagent and pCMV-p53mt135 plasmid or empty vector for 6 h. After transfection, cells resistant to neomycin were selected by incubating with medium containing 1 mg/mL G418 (geneticin) (Life Technologies), individual HeLa clones were isolated and tested for constitutive p53 expression. The p53-positive HeLa cells were selected and maintained in the presence of G418 (400 μg/mL), as were p53-negative control cells [27].

2.11 Statistical analysis

Data were expressed as mean ± SD. Statistical comparisons of the results were made using analysis of variance (ANOVA). Significant differences ($p < 0.05$) between the means of control and ISL-treated cells were analyzed by Dunnett's test.

3 Results

3.1 ISL inhibits cell proliferation and clonogenic survival in human cervical carcinoma cells

To investigate the potential cell proliferative inhibition activity of ISL in human cervical carcinoma cells, we first examined the effect of ISL on cell proliferation and clono-

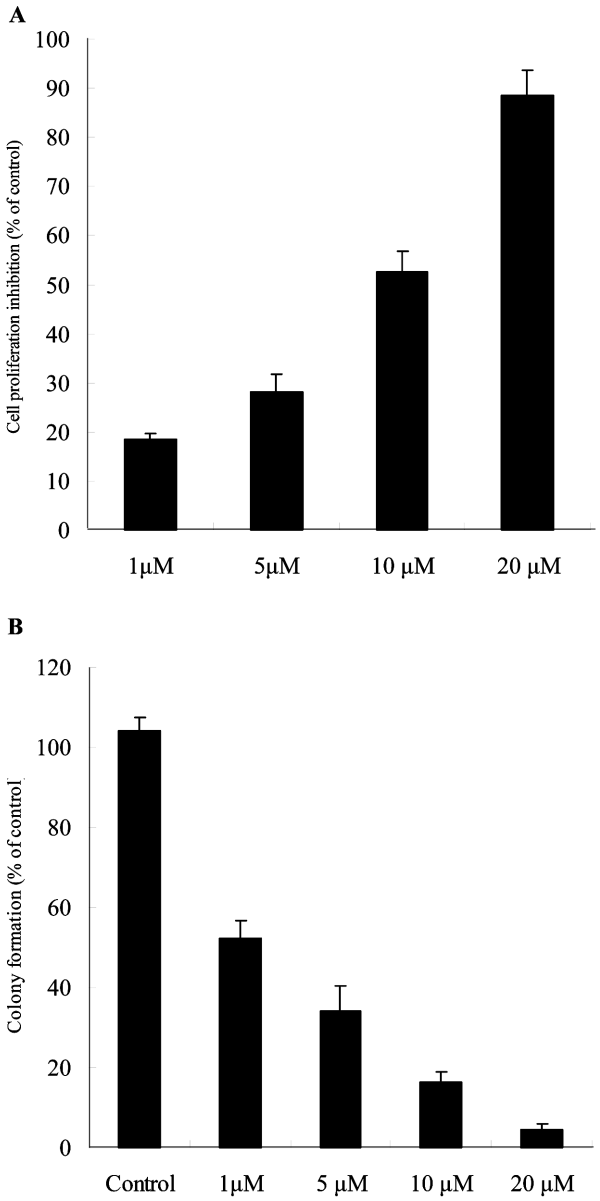

Figure 1. The inhibitory effects of ISL on cell proliferation inhibition and colony formation in human cervical carcinoma HeLa cells. (A) Inhibition effect of ISL on HeLa cell proliferation. (B) Influence of HeLa on the number of colony-forming cells, as evaluated by clonogenic assay. Cell growth inhibition activity of ISL was assessed by XTT. For colony-forming assay, the clonogenic assay was performed as described in Section 2. Results are expressed as the percentage of cell proliferation relative to the proliferation of control. The data shown are the mean from three independent experiments. Each value is the mean ± SD of three determinations.

genic survival in HeLa cells. As shown in Fig. 1A, exposure of HeLa cells to ISL for 48 h inhibited the growth of HeLa cells in a dose-dependent manner. The IC_{50} values of ISL were 9.8 μM.

The anticancer activities of ISL were assessed by clonogenic assays. HeLa cells showed the ability to form clones

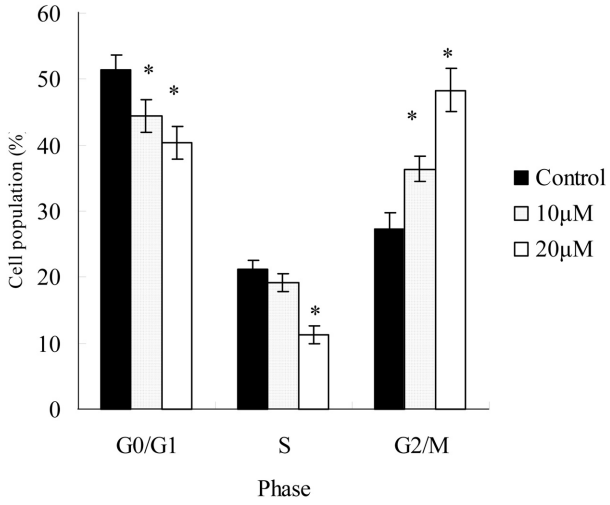

Figure 2. The effects of ISL on cell cycle distribution in HeLa cells. HeLa cells following treatment with vehicle alone (0.1% DMSO) and ISL (10 and 20 μM) for the indicated times were fixed and stained with PI, and cell cycle distribution was then analyzed by flow cytometry. The data indicate the percentage of cells in G0/G1, S, and G2/M phases of the cell cycle. Each value is the mean ± SD of three determinations. The asterisk indicates a significant difference between control and ISL-treated cells, as analyzed by Dunnett's test ($p < 0.05$).

in the untreated control wells. However, with the addition of ISL, a dose-dependent inhibition in clonogenicity was observed, with a >90% inhibition at a dosage of 20 μM ISL (Fig. 1B).

3.2 ISL-induced cell cycle arrest and apoptosis in HeLa cells

To investigate the mechanisms leading to loss of cell proliferation by ISL, we tested whether the observed inhibition effects of ISL on cell proliferation are due to induction of cell cycle arrest. As shown in Fig. 2, treatment of HeLa cells with 10 and 20 μM ISL increased the percentage of cells in the G2/M phase after 6 h exposure (Fig. 2).

We next assessed the effect of ISL on the induction of apoptosis in HeLa cells by DNA fragmentation assay. A quantitative evaluation was also made using TUNEL to detect DNA-strand breaks. Compared to vehicle-treated cells, ISL induced 24.3 and 39.5% of apoptotic cells in HeLa cells at concentrations of 10 and 20 μM at 48 h, respectively (Fig. 3A). TUNEL-positive cells were also made visible using a fluorescence microscope (Fig. 3B). Quantitative assessment of apoptosis was also assayed using a PI/Annexin V-FITC double. Compared with vehicle-treated cells, concentrations of 10 and 20 μM ISL induced 27.3 and 40.1% of the apoptotic HeLa cells at 48 h (Fig. 3C).

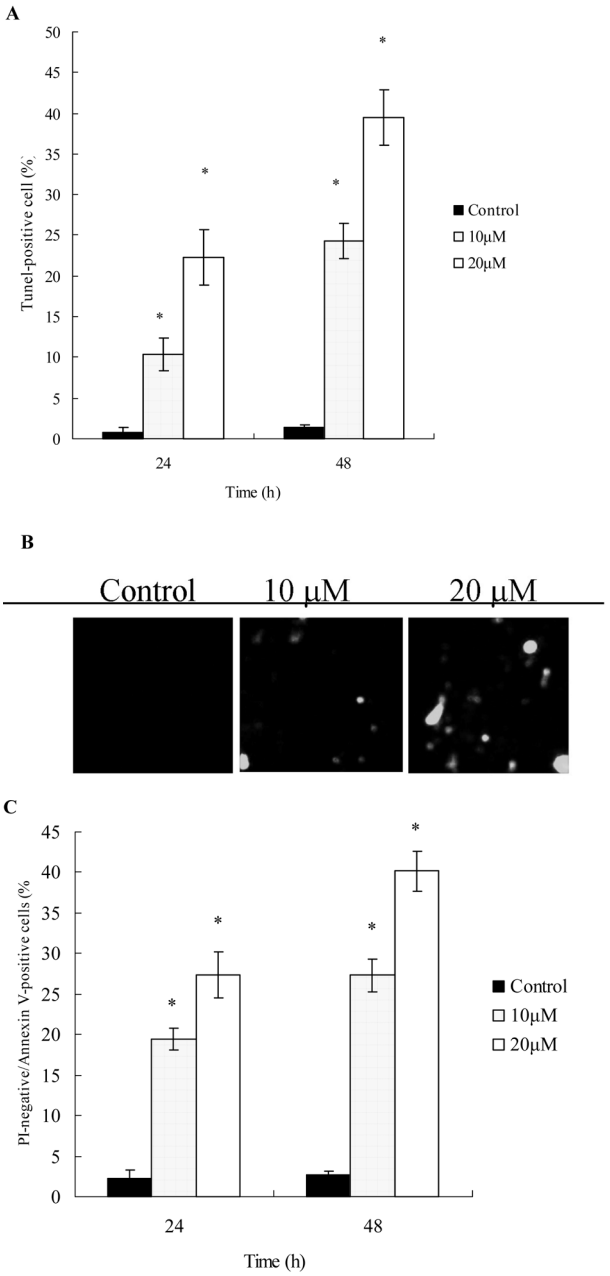

Figure 3. ISL induced apoptosis. Quantitative evaluations of TUNEL assay by flow cytometry (A) and fluorescence microscope (B). (C) The induction of apoptosis was assessed by Annexin V-FITC/PI dye. Cells were treated with 10 and 20 μM ISL for 24 or 48 h. PI-negative/Annexin V positive and TUNEL-positive cells were examined by flow cytometry. TUNEL-positive cells were observed by fluorescence microscope. Each value is the mean ± SD of three determinations. The asterisk indicates a significant difference between control and ISL-treated cells, as analyzed by Dunnett's test ($p < 0.05$).

3.3 The effect of ISL on G2/M phase-related factors

Because our studies showed that ISL treatment of HeLa cells results in G2/M phase cell cycle arrest, we examined the effect of ISL on cell cycle-regulatory molecules. We

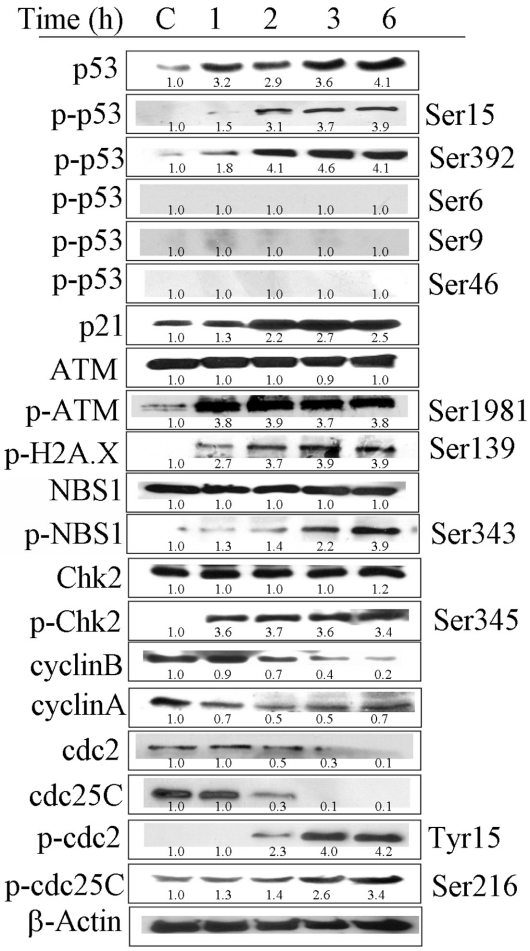

Figure 4. The effect of ISL in cell cycle-related factor. The levels of p53, phospho-p53, p21, ATM, phospho-ATM, phospho-H2A.X, phospho-NBS1, Chk2, phospho-Chk2, cyclin B, cyclin A, cdc2, cdc25C, phospho-cdc2, and phospho-cdc25C were assessed by immunoblot assay. Results shown are representative of three independent experiments. The intensity of the bands was determined by the SigmaGel software.

first assessed the status of p53 in ISL-treated HeLa cells. Exposure of cells to 20 μM ISL enhanced the phosphorylation of p53 on Ser15 and Ser392 (Fig. 4). Phosphorylation of p53 on Serine residues 6, 9, and 46 were undetectable. ISL treatment was also associated with an increase p53's downstream target, p21 (Fig. 4). Similarly, ISL caused a significant time-dependent increase in the phosphorylation (Ser1981) of ATM protein in cells. However, ISL treatment did not cause any change in the protein levels of total ATM. Exposure of HeLa cells to ISL resulted in increased levels of the phosphorylated (activated) form of H2A.X (Ser139) (a variant form of histone H2A) and NBS1 (Ser343), which are directly influenced by activated ATM kinase [9, 10] (Fig. 4). Furthermore, treatment of HeLa cells with 20 μM ISL resulted in rapid and sustained activation of Chk2 (phosphorylation at Ser345) (Fig. 4).

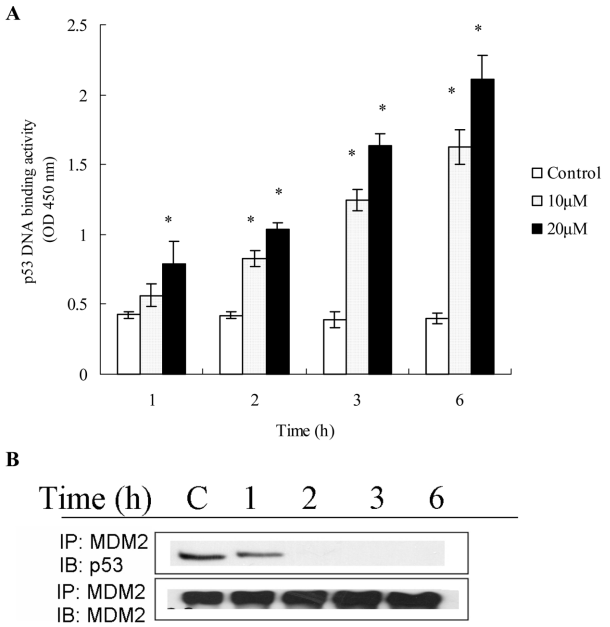

Figure 5. ISL increased the DNA binding activity and stability of p53. For (A), cells were treated with vehicle alone (0.1% DMSO) and ISL (10 and 20 μM) for the indicated times, and then DNA binding activity was assessed by TranAM p53 activity kit. For (B), the interaction of p53 with MDM2 was assessed by immunoprecipitation. Each value is the mean ± SD of three determinations. The asterisk indicates a significant difference between control and ISL-treated cells, as analyzed by Dunnett's test ($p < 0.05$).

ISL treatment of HeLa cells resulted in a time-dependent decrease in the protein expression of cyclin B, cyclin A, cdc2, and cdc25C (Fig. 4). In addition, exposure of these cells to ISL for 2 h resulted in increased levels of inactive phospho-cdc2 (Tyr15) and phospho-cdc25C (Ser216). Results from time-dependent studies have indicated that increasing phosphorylated Chk2 is followed by an increase in phospho-cdc25C, which in turn increased phospho-cdc2 (Fig. 4).

3.4 ISL decreases the interaction of p53 with MDM2

Previous studies have shown that the function and stability of p53 is principally regulated by phosphorylation at regulated by phosphorylation at various sites [12]. We assessed the DNA binding activity of p53 using to ELISA-based method, and the interaction of p53 with MDM2 by immunoprecipitation assay. As shown in Fig. 5A, ISL treatment resulted in the enhancement of p53 DNA binding activity. The enhancement of p53 transcriptal activity is correlated with the phosphorylation of p53 at Ser392. Furthermore, the association of p53 and MDM2 decreased in a time-dependent manner, which correlated with the phosphorylation of p53 at Ser15 (Fig. 5B).

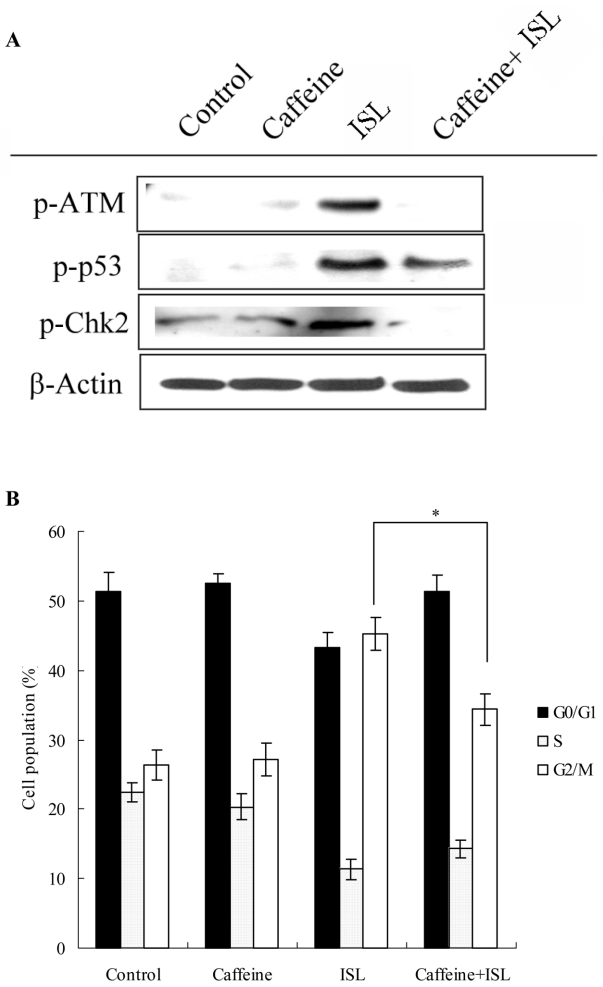

Figure 6. ATM inhibitor blocked ISL-mediated cell cycle arrest and phosphorylation of p53 and Chk2. For all blocking experiments, cells were incubated for 1 h in the presence or absence of 2.5 mM caffeine, then 20 μM ISL was added and incubated for 3 h for ATM, Chk2 and p53 phosphorylation (A) and 6 h for cell cycle analysis (B). Cell cycle distribution was assessed by flow cytometric analysis. Each value is the mean ± SD of three determinations. The asterisk indicates a significant difference between two test groups, as analyzed by Dunnett's test ($p < 0.05$).

3.5 The role of ATM on ISL-mediated cell cycle arrest

To verify the possible role of ATM in ISL-mediated G2/M arrest, HeLa cells were pretreated for 1 h with caffeine, a specific inhibitor for ATM. Subsequently, the inhibitor-treated cells were exposed to ISL, and then cell cycle distribution and associated events were examined. As shown in Fig. 6A, ISL-mediated ATM activation was effectively inhibited by 2.5 mM of caffeine. Flow cytometric analysis of HeLa cells exposed to ISL for 6 h showed that caffeine blocked ISL-mediated G2/M progression (Fig. 6B). In addition, pretreatment of cells with caffeine also decreased the

ISL-mediated phosphorylation of p53 (Ser15) and Chk2 (Fig. 6A).

3.6 The role of ATM on ISL-mediated cell cycle arrest and apoptosis

To further define the role of p53 in ISL-induced cell cycle arrest and apoptosis, we transfected pCMV-p53mt135 plasmid containing a gene encoding a dominant negative mutation of p53 that blocks normal p53 activity [27]. Overexpression of mutant p53 protein in cells transfected with the dominant negative p53 mutant plasmid was verified by immunoblot using antibodies for human p53 (recognizing both wild and mutant types of p53) (Fig. 7A). Cells expressing the p53 mutant were subsequently used to document ISL-mediated cell cycle arrest and apoptosis. As shown in Fig. 7B, the inhibition of p53 activity was accompanied by a reduction in the sensitivity of HeLa cells to ISL-mediated G2/M arrest. Furthermore, compared to vehicle-treated cells, induction of apoptosis by 20 μM ISL decreased from 36.3% in HeLa cells to 14.2% in p53 mutant cells after a 48 h treatment (Fig. 7C).

3.7 ISL induced apoptosis by initiation of mitochondrial pathway

To investigate the mitochondrial apoptotic events involved in ISL-induced apoptosis, we first analyzed the changes in the levels of the Bcl-2 family proteins. Immunoblot analysis showed that treatment of HeLa cells with ISL increased Bax and Bak protein levels (Fig. 8A). In contrast, ISL markedly decreased Bcl-2 levels, which led to an increase in the Bax/Bcl-2 ratio (Fig. 8A). Additionally, ISL also decreased the expression of Bcl-X_L. These effects of ISL on the Bcl-2 family proteins resulted in the decrease of mitochondrial membrane potential in HeLa cells (Fig. 8B).

One of the hallmarks of the apoptotic process includes the activation of cysteine proteases, which represent both initiators and executors of cell death. Upstream caspase-9 activities also increase significantly when HeLa cells are treated with ISL (Fig. 8C). Furthermore, when cells are pretreated with the specific caspase-9 inhibitor LEHD-CHO before ISL treatment, the apoptosis induction effect of ISL was decreased in HeLa cells (Fig. 8D).

4 Discussion

Uterine cervical cancer is the most common neoplasm of women in both developed and developing countries [1 – 4]. In our study, we have found that ISL effectively inhibits tumor cell growth concomitant with induction of cell cycle arrest and apoptosis.

Tumor suppressor gene p53 is a key element in the induction of cell cycle arrest and apoptosis following DNA dam-

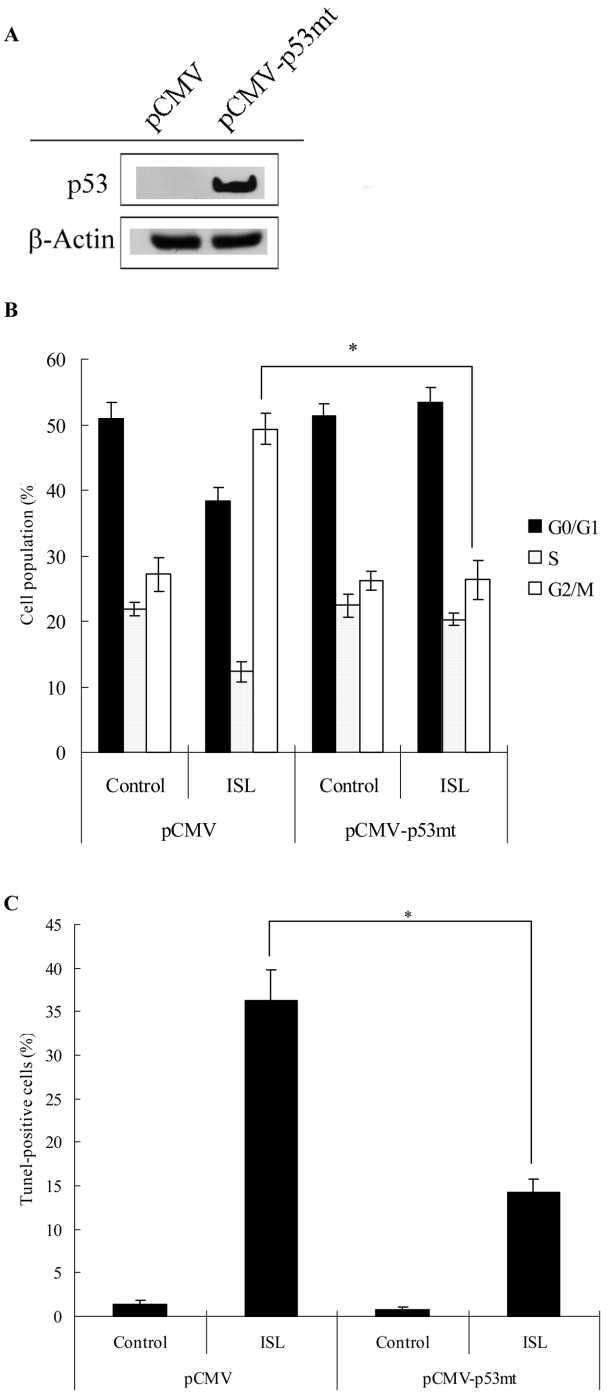

Figure 7. Effect of p53 inhibition on ISL-mediated cell cycle arrest and apoptotic cell death. (A) The expression of p53mt in stable pCMV-p53mt transfected HeLa cells. The p53 inhibition decreased the effect of ISL on cell cycle arrest (B) and apoptosis induction (C). HeLa cells and mutant p53-transfected HeLa cells were treated with 20 μM ISL for 6 h (cell cycle assay) and 48 h (apoptosis assay). The induction of apoptosis was determined by TUNEL analysis. Each value is the mean ± SD of three determinations. The asterisk indicates a significant difference between two test groups, as analyzed by Dunnett's test ($p < 0.05$).

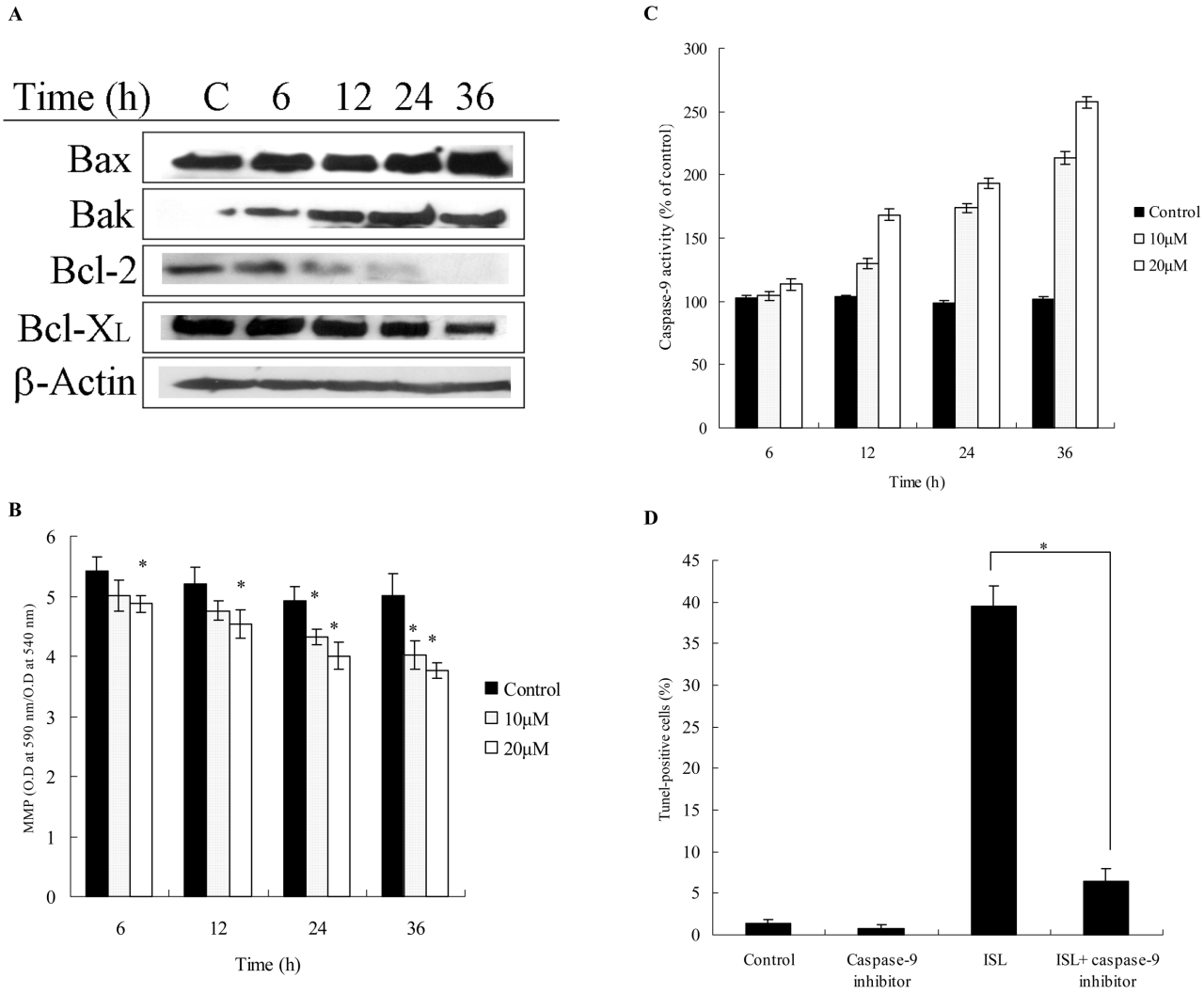

Figure 8. ISL induces apoptosis through the mitochondrial apoptotic pathway. (A) The effect of ISL on expression of the Bcl-2 family protein. (B) ISL caused a decrease of mitochondrial membrane potential, but (C) increased caspase-9 activation. (D) Caspase-9 inhibitor decreased ISL-induced apoptosis. The levels of Bcl-2 family proteins were assessed by immunoblot assay. The $\Delta\Psi m$ was measured by JC-1 staining. Caspase-9 activity was measured by caspase-9 activity assay kit. For caspase-9 inhibitor blocking experiments, cells were preincubated with LEHD-CHO (20 μM) for 1 h before the addition of 20 μM ISL for an additional 48 h. Each value is the mean ± SD of three determinations. The asterisk indicates a significant difference between control and ISL-treated cells, as analyzed by Dunnett's test ($p < 0.05$).

age or cellular stress in human cells [12, 28]. Cell-cycle arrest dependent on p53 requires transactivation of p21 or other cell cycle-related factors [29]. The induction of p21 causes subsequent arrest in the G0/G1 or G2/M phase of the cell cycle by binding of the cyclin–cdk complex [30, 31]. In this study, we have shown that treatment of HeLa cells with ISL resulted in the accumulation of p53 and phospho-p53 (Ser15). We have also found that suppression of normal p53 activity *via* dominant-negative p53 decreased ISL-induced G2/M arrest, suggesting that p53 play an important role in ISL-triggered cell cycle checkpoint. Indeed, we also have found that ISL decreases the expression of cyclin B, cyclin A, cdc25C, and cdc2, while it increases the amount of p21 and phosphorylation of cdc2, phospho-cdc25C, and phospho-Chk2. Our results show that ISL induces phosphorylation of cdc25C (Ser216) through Chk2 activation, and remains cdc25C inactive. Further downstream, inactivated cdc2 was not dephosphorylated by cdc25C. Therefore, cdc2 accumulated in an inactive phosphorylated state (Tyr15), resulting in cells that were unable to proceed through the mitotic phase. These data suggest that ISL may prove to be a valuable tool for inhibition of cdc2/cyclin B and cdc2/cyclin A complex in cervical cancers for the following reasons: (i) the down-regulation of cyclin B and cyclin A by ISL, (ii) the induction of p21 by ISL in a p53-dependent manner, which may subsequently inhibit the

function of cdc2, and (iii) the increase of activated Chk2 followed by an increase in inactivated phospho-cdc25C and phospho-cdc2, suggesting that increased cdc25C phosphorylation by Chk2 may also decrease functioning phosphatase for dephosphorylating and activating cdc2.

ATM pathway has been demonstrated to associate with the trigger of cell cycle checkpoint by both DNA damage-dependent and independent manners [7–9, 32]. Once activated, ATM phosphorylates various downstream molecules such as p53, MDM2, Chk1, Chk2, H2A.X, and Nijmegen breakage syndrome (NBS1), resulting in cell cycle arrest or cell death [9–11]. Phosphorylated NBS1 is an adaptor molecule for ATM-dependent phosphorylation of Chk2, which phosphoryaltes the cdc25 phosphatase and is responsible for S and G2/M phase checkpoints [7, 8, 33–35]. ATM phosphorylates p53 at Ser15, resulting in prolongation of p53 half-life by inhibiting p53–MDM2 complex formation [36, 37]. In this report, we have shown that treatment of HeLa cells with ISL resulted in the accumulation of phospho-ATM at Ser1981. This ATM activation correlated well with the ISL-induced increase of H2A.X and NBS1 phosphorylation. Furthermore, we observed that blocking the ISL-induced activation of ATM by the specific inhibitor caffeine could prevent p53 phosphorylation (Ser15), suggesting that ISL-induced ATM activation contributes to the stabilization of p53 function by Ser15 phosphorylation, which decreases the interaction of p53 and MDM2. In addition, our results showed that exposure of HeLa cells to ISL led to a concurrent phosphorylation of Chk2, whereas caffeine pretreatment inhibited Chk2 phosphorylation, suggesting that the activation of ATM induced by ISL is involved in the activation of Chk2. Moreover, the ATM inhibitor caffeine prevented ISL-induced G2/M arrest, further suggesting that cooperation of ATM with Chk2 and the p53-dependent pathway plays a crucial role in ISL-induced G2/M arrest.

Mitochondrial apoptotic pathway has been described as an important signaling of apoptotic cell death for mammalian cells [38, 39]. Following the treatment of HeLa cells with ISL, we observed that ISL treatment resulted in a significant increase of Bax and Bak expression, and a decrease of Bcl-2 and Bcl-X_L, suggesting that changes in the ratio of the proapoptotic and antiapoptotic Bcl-2 family proteins might contribute to the apoptosis-promotion activity of ISL. Our finding also showed a collapse of $\Delta\Psi m$, and the activation of caspase-9 after HeLa cells were treated with ISL. These mitochondrial apoptotic events are correlated with the modulation of ISL on Bcl-2 family proteins. These results confirm that ISL-induced apoptosis is associated with regulation of Bcl-2 family proteins.

In conclusion, the present study demonstrated that: (i) human uterine cervical cancer HeLa cells are highly sensitive to growth inhibition by ISL, (ii) reduced survival of HeLa cells after exposure to ISL is associated with G2/M phase cell cycle arrest and induction of apoptosis, (iii) ISL can inhibit cell cycle progression at the G2/M phase by increasing p21 expression in a p53-dependent manner, and by decreasing the expression of cdc2, cdc25C, and cyclin B, (iv) ISL-induced cell growth inhibition in the HeLa cells is mediated by activation of ATM, which stabilizes p53 by phosphorylation of p53 at Ser15, and by decreasing the interaction of p53 and MDM2, (v) ISL-mediated ATM activation also phosphorylates Chk2 and subsequently increases the accumulation of inactive cdc25C and cdc2, and (vi) ISL finally trigger mitochondrial apoptotic pathway by regulation of the Bcl-2 family protein expression. These findings suggest that ISL may be a promising chemopreventive agent in the fight against human uterine cervical cancer.

We thank the Division of Research Resource, Department of Medical Research, Kaohsiung Medical University Hospital for providing experiment space and experimental instruments.

The authors have declared no conflict of interest.

5 References

[1] Tsukamoto, H., Shibata, K., Kajiyama, H., Terauchi, M., *et al*., Aminopeptidase N (APN)/CD13 inhibitor, Ubenimex, enhances radiation sensitivity in human cervical cancer, *BMC Cancer* 2008, *8*, 74.

[2] Waqqoner, S.-E., Cervical cancer, *Lancet* 2003, *361*, 2217–2225.

[3] Inoue, T., Prognostic significance of the depth of invasion relating to nodal metastases, parametrial extension, and cell types. A study of 628 cases with Stage IB, IIA, and IIB cervical carcinoma, *Cancer* 1984, *54*, 3035–3042.

[4] Thomas, G.-M., Improved treatment for cervical cancer–concurrent chemotherapy and radiotherapy, *N. Engl. J. Med*. 1999, *340*, 1198–1200.

[5] Sultana, H., Kigawa, J., Kanamori, Y., Itamochi, H., *et al*., Chemosensitivity and p53-Bax pathway-mediated apoptosis in patients with uterine cervical cancer, *Ann. Oncol*. 2003, *14*, 214–219.

[6] Bruno, T., De Nicola, F., Iezzi, S., Lecis, D., *et al*., Che-1 phosphorylation by ATM/ATR and Chk2 kinases activates p53 transcription and the G2/M checkpoint, *Cancer Cell* 2006, *10*, 473–486.

[7] Roos, W.-P., Kaina, B., DNA damage-induced cell death by apoptosis, *Trends Mol. Med*. 2006, *12*, 440–450.

[8] Lavin, M.-F., Kozlov, S., ATM activation and DNA damage response, *Cell Cycle* 2007, *6*, 931–942.

[9] Hunt, C.-R., Pandita, R.-K., Laszlo, A., Higashikubo, R., *et al*., Hyperthermia activates a subset of ataxia-telangiectasia mutated effectors independent of DNA strand breaks and heat shock protein 70 status, *Cancer Res*. 2007, *67*, 3010–3017.

[10] Dornan, D., Shimizu, H., Mah, A., Dudhela, T., *et al*., ATM engages autodegradation of the E3 ubiquitin ligase COP1 after DNA damage, *Science* 2006, *313*, 1122–1126.

[11] Stiff, T., O'Driscoll, M., Rief, N., Iwabuchi, K., *et al*., ATM and DNA-PK function redundantly to phosphorylate H2AX after exposure to ionizing radiation, *Cancer Res*. 2004, *64*, 2390 – 2396.

[12] Ryan, K.-M., Phillips, A.-C., Vousden, K.-H., Regulation and function of the p53 tumor suppressor protein, *Curr. Opin. Cell Biol*. 2001, *13*, 332 – 337.

[13] Soussi, T., p53 alterations in human cancer: More questions than answers, *Oncogene* 2007, *26*, 2145 – 2156.

[14] Kulikov, R., Winter, M., Blattner, C., Binding of p53 to the central domain of Mdm2 is regulated by phosphorylation, *J. Biol. Chem*. 2006, *281*, 28575 – 28583.

[15] Pospísilová, S., Brázda, V., Kucharíková, K., Luciani, M.-G., *et al*., Activation of the DNA-binding ability of latent p53 protein by protein kinase C is abolished by protein kinase CK2, *Biochem. J*. 2004, *378*, 939 – 947.

[16] Vaya, J., Belinky, P. A., Aviram, M., Antioxidant constituents from licorice roots: Isolation, structure elucidation and antioxidative capacity toward LDL oxidation, *Free Radic. Biol. Med*. 1997, *23*, 302 – 313.

[17] Chan, S.-C., Chang, Y.-S., Wang, J.-P., Chen, S.-C., Kuo, S.-C., Three new flavonoids and antiallergic, anti-inflammatory constituents from the heartwood of *Dalbergia odorifera*, *Planta Med.* 1998, *64*, 153 – 158.

[18] Tawata, M., Aida, K., Noguchi, T., Anti-platelet action of isoliquiritigenin, an aldose reductase inhibitor in licorice, *Eur. J. Pharmacol*. 1992, *212*, 87 – 92.

[19] Baba, M., Asano, R., Takigami, I., Takahashi, T., *et al*., Studies on cancer chemoprevention by traditional folk medicines XXV. Inhibitory effect of isoliquiritigenin on azoxymethane-induced murine colon aberrant crypt focus formation and carcinogenesis, *Biol. Pharm. Bull*. 2002, *25*, 247 – 250.

[20] Yamazaki, S., Morita, T., Endo, H., Hamamoto, T., *et al*., Isoliquiritigenin suppresses pulmonary metastasis of mouse renal cell carcinoma, *Cancer Lett.* 2002, *183*, 23 – 30.

[21] Kanazawa, M., Satomi, Y., Mizutani, Y., Ukimura, O., *et al*., Isoliquiritigenin inhibits the growth of prostate cancer. *Eur. Urol*. 2003, *43*, 580 – 586.

[22] Maggiolini, M., Statti, G., Vivacqua, A., Gabriele, S., *et al*., Estrogenic and antiproliferative activities of isoliquiritigenin in MCF7 breast cancer cells, *J. Steroid Biochem. Mol. Biol*. 2002, *82*, 315 – 322.

[23] Ma, J., Fu, N.-Y., Pang, D.-B., Wu, W.-Y., Xu, A.-L., Apoptosis induced by isoliquiritigenin in human gastric cancer MGC-803 cells, *Planta Med.* 2001, *67*, 754 – 757.

[24] Iwashita, K., Kobori, M., Yamaki, K., Tsushida, T., Flavonoids inhibit cell growth and induce apoptosis in B16 melanoma 4A5 cells, *Biosci. Biotechnol. Biochem*. 2000, *64*, 1813 – 1820.

[25] Hsu, Y.-L., Kuo, P.-L., Chiang, L.-C., Lin, C.-C., Isoliquiritigenin inhibits the proliferation and induces the apoptosis of human nonsmall cell lung cancer a549 cells, *Clin. Exp. Pharmacol. Physiol*. 2004, *7*, 414 – 418.

[26] Hsu, Y.-L., Kuo, P.-L., Lin, C.-C., Isoliquiritigenin induces apoptosis and cell cycle arrest through p53-dependent pathway in Hep G2 cells, *Life Sci*. 2005, *77*, 279 – 292.

[27] Hsu, Y.-L., Cho, C.-Y., Kuo, P.-L., Huang, Y.-T., Lin, C.-C., Plumbagin (5-hydroxy-2-methyl-1,4-naphthoquinone) induces apoptosis and cell cycle arrest in A549 cells through p53 accumulation *via* c-Jun NH2-terminal kinase-mediated phosphorylation at serine 15 *in vitro* and *in vivo*, *J. Pharmacol. Exp. Ther*. 2006, *318*, 484 – 494.

[28] Vousden, K.-H., Lane, D.-P., p53 in health and disease, *Nat. Rev. Mol. Cell Biol*. 2007, *8*, 275 – 283.

[29] Kosakowska-Cholody, T., Cholody, W.-M., Monks, A., Woynarowska, B.-A., Michejda, C.-J., WMC-79, a potent agent against colon cancers, induces apoptosis through a p53-dependent pathway, *Mol. Cancer Ther*. 2005, *4*, 1617 – 1627.

[30] Child, E.-S., Mann, D.-J., The intricacies of p21 phosphorylation: Protein/protein interactions, subcellular localization and stability, *Cell Cycle* 2006, *5*, 1313 – 1319.

[31] Gartel, A.-L., Radhakrishnan, S.-K., Lost in transcription: p21 repression, mechanisms, and consequences, *Cancer Res*. 2005, *65*, 3980 – 3985.

[32] Matsuoka, S., Ballif, B.-A., Smogorzewska, A., McDonald, E. R., III *et al*., ATM and ATR substrate analysis reveals extensive protein networks responsive to DNA damage, *Science* 2007, *316*, 1160 – 1166.

[33] Brown, K.-D., Rathi, A., Kamath, R., Beardsley, D.-I., *et al*., The mismatch repair system is required for S-phase checkpoint activation, *Nat. Genet.* 2003, *33*, 80 – 84.

[34] Kuo, P.-L., Hsu, Y.-L., Cho, C.-Y., Plumbagin induces G2-M arrest and autophagy by inhibiting the AKT/mammalian target of rapamycin pathway in breast cancer cells, *Mol. Cancer Ther*. 2006, *5*, 3209 – 3221.

[35] Singh, S.-V., Herman-Antosiewicz, A., Singh, A.-V., Lew, K.-L., *et al*., Sulforaphane-induced G2/M phase cell cycle arrest involves checkpoint kinase 2-mediated phosphorylation of cell division cycle 25C, *J. Biol. Chem*. 2004, *279*, 25813 – 25822.

[36] Hideshima, T., Mitsiades, C., Akiyama, M., Hayashi, T., *et al*., Molecular mechanisms mediating antimyeloma activity of proteasome inhibitor PS-341, *Blood* 2003, *101*, 1530 – 1534.

[37] Lee, Y.-S., Wan, J., Kim, B.-J., Bae, M.-A., Song, B.-J., Ubiquitin-dependent degradation of p53 protein despite phosphorylation at its N terminus by acetaminophen, *J. Pharmacol. Exp. Ther*. 2006, *317*, 202 – 208.

[38] Kuo, P.-L., Chen, C.-Y., Hsu, Y.-L., Isoobtusilactone A induces cell cycle arrest and apoptosis through reactive oxygen species/apoptosis signal-regulating kinase 1 signaling pathway in human breast cancer cells, *Cancer Res*. 2007, *67*, 7406 – 7420.

[39] Schwarz, M., Andrade-Navarro, M.-A., Gross, A., Mitochondrial carriers and pores: Key regulators of the mitochondrial apoptotic program? *Apoptosis* 2007, *12*, 869 – 876.